Structured Learning of a Nonlinear Dynamic System Component for Vehicle Motion Simulation

Matthew C Best, Andrew P Newton (Loughborough University, UK)

Dept Aeronautical and Automotive Engineering
Loughborough University, Leicestershire, LE11 3TU, UK
Phone: +44 1509 227209
Fax: +44 1509 227275
E-mail M.C.Best@lboro.ac.uk

Here we consider the design of a general subsystem model which is required to operate in series with the known dynamics of a plant or actuator, to achieve a desired overall system response. The example model is used in series with a motion platform to emulate vehicle handling dynamics. The method works in stages, first isolating the required linear response by fitting a frequency response function, then modelling this with a fixed order linear system in modal canonical form. A nonlinear saturation is then optimised for each modal state. The results are demonstrated for simulated and vehicle test data, and these achieve the principal objectives, of low state and parameter order. Some limitations to the method emerge – principally that there remain challenges to extension of the model to multi-input / output operation.

Vehicle Dynamics and Control, Integrated Motion Control, Modeling and Simulation Technology, Virtual Reality

Principal Notation

a_y	lateral acceleration (m/s^2)
$\dot{r}$	yaw acceleration (rad/s^2)
δ	steer angle input (rad)
Φ, ϕ	Identified vehicle model subsystem, fully nonlinear and linearised models respectively.
Ψ, ψ	Target vehicle system, fully nonlinear and linearised approximation respectively
$g(j\omega)$	Linear approximation to rig / actuator system
n	order of identified model
f_i	nonlinear function applied to i^{th} state in Φ
p_i, β_i	parameters defining nonlinear function f_i
λ_i (σ_i+jω_i)	eigenvalues, input and output coefficients
b_i, c_i, d_i	of canonical state space model ϕ
L	subscript denoting a system response to low magnitude inputs, suited to simulation by a linear model
NL	subscript denoting a system response to higher magnitude inputs, suited to simulation by a nonlinear model

1. INTRODUCTION

Recent acquisition of a six strut moving platform vehicle simulator at Loughborough University has prompted consideration of the most suitable vehicle model to emulate correct vehicle accelerations, within the motion constraints of the platform. Motion platforms typically employ washout filters to control the limits of excursion, but these also apply dynamic distortion and lag. The best model would thus interface directly between steering wheel / pedals and motion, providing platform accelerations ($\underline{a}$) such that the combined dynamics of model and actuation provide the required response. The input / output relationship is illustrated in Fig. 1; the object is to determine which dynamic system Φ will achieve the best match in responses $\underline{a}$ for a known platform plant g.

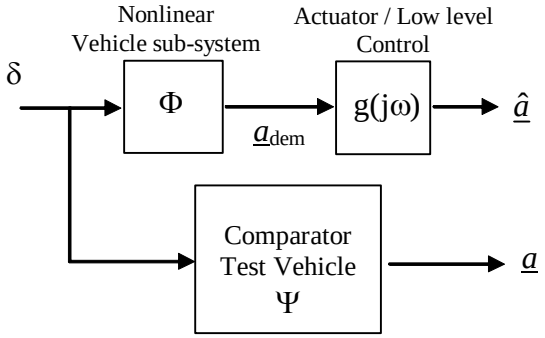

Fig. 1 System composition compared with vehicle

The solution for Φ might be achieved by combining a vehicle model of suitable complexity with an approximated inverse of the simulator plant. However that approach has disadvantages in identifying the plant inverse, but also in what constitutes 'suitable' for the model, given real-time processing constraints, and also the problem of identifying (eg tyre properties for) the vehicle model. A solution is sought, which

combines :

i. identification of model parameters
ii. determination of the required model order
iii. provision of a nonlinear solution
iv. no separate inversion of the motion control plant
v. training to a given input / output combination, but with the ability to safely, and ideally accurately, react to other inputs

Φ will clearly not, in isolation, represent vehicle dynamics, so a physics-based model is not warranted. The obvious approach is to employ a neural network, but this does not address points (ii) and (v) above; in particular, such a solution presents the issue of potentially extreme, unsafe, and certainly dynamically unpredictable responses, when presented with inputs which are different from the design scenario. Instead, the approach examined here considers a novel staged approach, to first determine the modes required in a linearisation of Φ, and then augment this system, in modal canonical form with one nonlinear function for each state. The aim is to introduce the required nonlinearity with a minimum of additional parameters; these can then be optimised to maximise accuracy in the combined system output set $\underline{a}$ for a preselected set of test inputs δ.

The proposed structure deliberately separates linear and nonlinear components, with the final stage nonlinear optimisation shaping simple saturation functions. This should result in a suitably general model / plant combination. The identification process can also be carried out rapidly, without use of the simulator rig, so various model order choices can be tested to establish a suitable trade-off between complexity and accuracy.

2. IDENTIFICATION ALGORITHM

The structure of the model subsystem Φ is illustrated for a single input, three state and two output example, in figure 2.

The boxed linear system is quartered to show the overall continuous state-space structure,

$$\left[\begin{array}{c|c} \mathbf{A} & \mathbf{B} \\ \hdashline \mathbf{C} & \mathbf{D} \end{array}\right]$$

within which the linearisation of Φ, which we will term ϕ, is shown in canonical form. With this structure, each nonlinear element multiplies a separate state, and because these are modally independent there is no anticipated need for further parameters to distribute the nonlinearity back to the state derivatives.

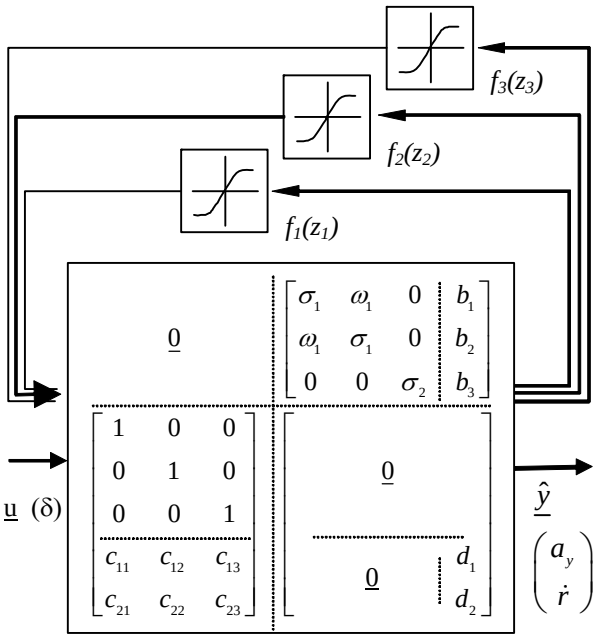

Fig. 2 Subsystem (Φ) structure, based around modal canonical linear state space model

Each nonlinear element is modelled here by

$$f = p\sin\left(\beta \tan^{-1}\left(\frac{z}{p\beta}\right)\right) \qquad (1)$$

a reduced form of Pacejka's magic formula, chosen to allow variation in peak through the setting of p, and shape variation through β, yet constraining f such that $\frac{\partial f}{\partial z} = 1$; thus for low magnitude variations in $\underline{z}$, the system equates to the prescribed linear form.

2.1 Linear Model Identification in the Frequency Domain

The identification is focused on a key single input / output relationship, in this example the lateral acceleration response, a_y, to steer input δ. The simulator plant dynamics are first identified by recording the acceleration response to an acceleration demand applied to the motion cueing system. A gaussian white noise input

$$a_{y\mathrm{dem}} = N\left(0, \sigma^2\right), \quad \sigma = 1\mathrm{m/s}^2 \qquad (2)$$

is used, and the response is recorded using an accelerometer mounted on the motion platform. 300 seconds of this signal were recorded at a sampling rate of 1kHz, and Welch's averaged periodogram method [1] was used, with a Hanning window length T = 30 seconds to find the frequency response function $g(j\omega)$ (see Matlab function `tfe`). This is illustrated in Fig. 3.

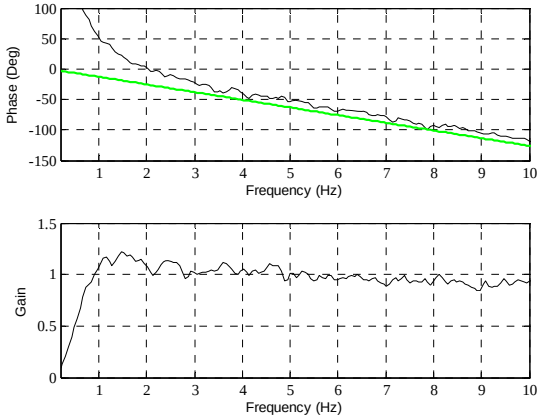

Fig. 3 Identified frequency response function $g(j\omega)$

We can see by inspection that this response closely approximates a constant time delay (grey line),

$$g(j\omega) = e^{-j\omega\tau}, \text{ where } \tau = 0.04\text{s} \qquad (3)$$

As the windowing method corrupts the lower frequencies in the response, and equation (3) allows easier adjustment of measured responses $\underline{a}$ for comparison of results, this simplification is adopted for the remainder of this study. (Though note that any form of simplification is not a *requirement* of the method.)

Now, if a similar process of linear model identification is conducted on the test vehicle, the response function $\psi(j\omega)$ can be derived between δ and a_y. In practice, this involves testing on a wide straight section of proving ground, with the vehicle at constant speed and the driver applying random steer input with as high a bandwidth as can reasonably be achieved – typically max 4-6Hz. Welch's method then yields a response $\psi(j\omega)$ which can be combined with $g(j\omega)$ to provide an estimate of the required linear behaviour in Φ :

$$\phi(j\omega) = \frac{\psi(j\omega)}{g(j\omega)} \qquad (4)$$

Fig. 4 shows how this has been done for the simulated test vehicle Ψ described in Section 3, with both $\psi(j\omega)$ and $\phi(j\omega)$ illustrated by the thicker, grey lines.

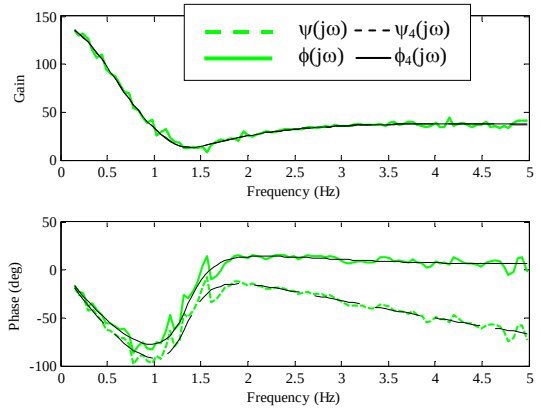

Fig. 4 Simulated identification of frequency response functions $\psi(j\omega)$ and $\phi(j\omega)$

2.2 State space formulation

For a given model order *n*, the coefficients b' and a' for a linear time-invariant transfer function

$$\phi_n(s) = \frac{b'_n s^n + \cdots b'_1 s + b'_0}{a'_n s^n + \cdots a'_1 s + a'_0} \qquad (5)$$

can be approximated. With s=jω, the cost function

$$\left|\phi_n(j\omega) - \phi(j\omega)\right|^2 \qquad (6)$$

is applied, and the coefficients are identified by an iterative search using a damped Gauss-Newton method [2] (see Matlab function `invfreqs`). The accuracy of fit for $\phi_n(s)$ is clear by examining $\phi_n(j\omega)$ – eg for $n = 4$ the result is excellent for the simulated example in Fig. 4.

The system is converted to state-space form, and then to modal canonical form by transforming the states using the eigenvector matrix (see Matlab function `canon`) to provide the required form

$$\begin{aligned} \dot{\underline{z}} &= \left[\underline{\lambda}\right]\underline{z} + \underline{b}\delta \\ a_y &= \underline{c}^T\,\underline{z} + d\,\delta \end{aligned} \qquad (7)$$

Finally to complete the linear model, any further outputs can be fitted by ordinary least squares regression to establish further elements c_i, d_i. This is done by simulation of the modal states $\underline{z}$ on the test inputs δ which were used to determine $\psi(j\omega)$, and for which records of the further outputs are also available. Denoting those inputs and states δ_ψ, $\underline{z}_\psi$ respectively, the secondary outputs (eg yaw acceleration $\dot{r}$) can be modelled as

$$\left[\begin{array}{c}\underline{c}_{\dot{r}} \\ \hdashline d_{\dot{r}}\end{array}\right] = \left(U^T U\right)^{-1} U^T \dot{r}(t) \qquad (8)$$

where $U = \left[\underline{z}_\psi^T(t) \;\vdots\; \delta_\psi(t)\right]$

Of course within this process, any secondary output must encounter similar filtering by the rig actuation / low level control; this is the case for all six degrees of freedom of the rig in question however, since all motion is governed through a combination of strut motions in a Stewart platform.

2.3 Nonlinear Component Identification

The linear model is now in a form to occupy elements $\underline{\lambda}$, $\underline{b}$, $\underline{c}$ and $\underline{d}$ in Fig. 2, and to complete the subsystem Φ, an optimisation is required to identify the remaining nonlinearity coefficients $\underline{p}$ and $\underline{\beta}$. The cost function to achieve this is based on output errors $(\hat{a} - a)$ but will also need to establish a trade-off between retaining performance in the linear $_{(L)}$ region and achieving performance in the nonlinear $_{(NL)}$ region. Therefore an aggregated scalar cost is evaluated over two responses;

$$P = trace\left(W^2\left(\left|\underline{\hat{a}}_{NL}(t) - \underline{a}_{NL}(t)\right|^2 + \left|\underline{\hat{a}}_{L}(t) - \underline{a}_{L}(t)\right|^2\right)\right) \qquad (9)$$

Where $\underline{a}_L$ is a section of the random-steer test vehicle response used in Section 2.1 and $\underline{a}_{NL}$ is the vehicle response from a more aggressive manoeuvre; $\underline{a}_{NL}$ might be a specific test such as a J-turn or lane-change manoeuvre, for which the simulator is required to respond as accurately as possible. W then provides a diagonal weighting matrix to regulate the relative magnitude / importance of the outputs. The relative lengths of the two responses $_{\mathrm{L}}$ and $_{\mathrm{NL}}$ can also be adjusted to weight the influence of the f_{i}.

The cost is minimised using a constrained sequential quadratic programming algorithm [3] which operates on numerical estimates of the Hessian of the Lagrangian (see Matlab function `fmincon`).

3. SIMULATION EXPERIMENT

The algorithm is tested in simulation by employing a bicycle model for Ψ, viz

$$\begin{aligned} \dot{v} &= \frac{F_{yf} + F_{yr}}{M} - ur \\ \dot{r} &= \frac{bF_{yf} - cF_{yr}}{I_{zz}} \end{aligned} \qquad (10)$$

where the tyre forces F_y are determined from the simple four parameter Pacejka magic formula [4] as a function of load dependent cornering stiffness and peak force, and with the loads accounting for lateral transfers. Critically, the model also includes appropriate tyre relaxation delays – here modeled by first order lag terms each with time constant 15ms; without these, $\phi_n(s)$ would be non-causal, given its requirement to compensate rig acceleration delays. The forward speed is set to 15m/s, and the tyre model structure is more fully described in [5].

Accepting $g(j\omega)$ as in equation (3), and that this applies to all relevant output accelerations (Section 2.2), the function $\psi_n(s)$ can be optimised to either of the two outputs a_y, $\dot{r}$ which we will consider here – the proviso is that a simple enough fundamental modal relationship exists which is common to both – this is certainly the case for the bicycle model.

The result of optimising $\psi_2(s)$ and $\psi_4(s)$ for δ to $\dot{r}$, and then using equation (8) to fit an output relationship between $\underline{z}_\psi$ and a_y is shown in Fig. 5. (This is essentially the opposite order of process to that described in Section 2, but was found to yield better results.)

Naturally, the fit to $\dot{r}$ is better than to a_y, though note how accurately the time hisotries match, with the case $n = 4$ compensating the rig delay almost perfectly, in both outputs.

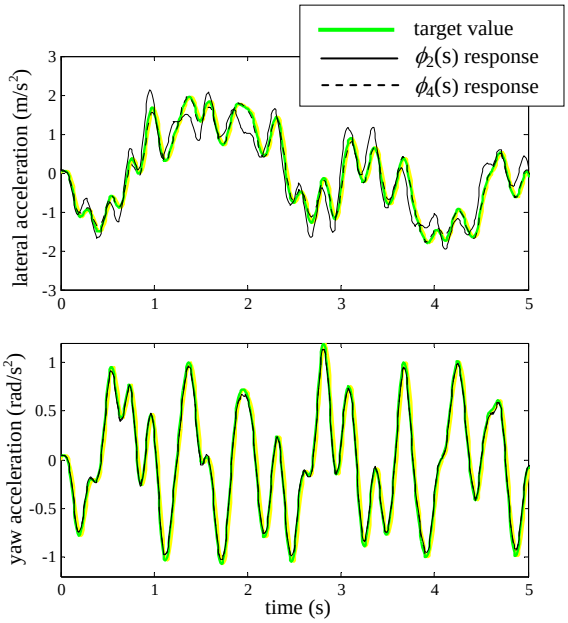

Fig. 5 Performance of $\phi_2(s)$ and $\phi_4(s)$ on a representative section of linear test $\underline{a}_L$.

The identified eigenvalues are

$$\begin{aligned} \text{for } n = 2, \quad \lambda &= \left[-7.8 \pm 1.5\,j\right] \\ \text{for } n = 4, \quad \lambda &= \begin{bmatrix} -22.9 \pm 33.5\,j \\ -5.1 \pm 2.4\,j \end{bmatrix} \end{aligned} \qquad (11)$$

Fig. 6 shows the nonlinear test, a series of step steer events, δ = 3° to the right, followed by 2° left and finally 1° right. The linear system response is compared with that of the completed system Φ, in this case carrying forward the n = 4 result; the nonlinear functions $f_1 - f_4$ which achieve this are illustrated in Fig. 7.

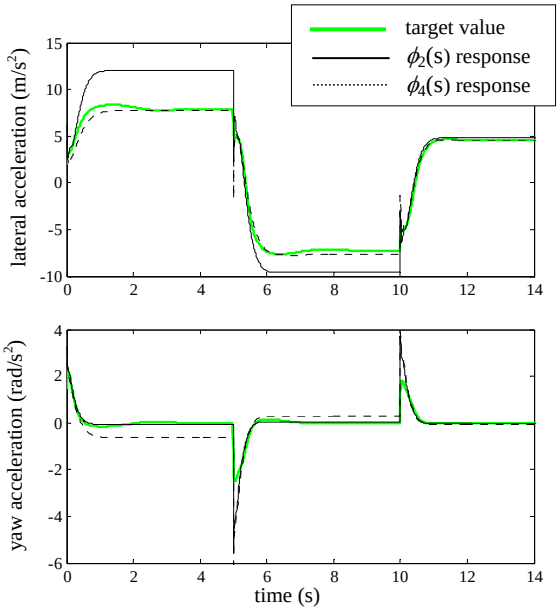

Fig.6 Performance of $\Phi_4(s)$ on nonlinear test $\underline{a}_{NL}$

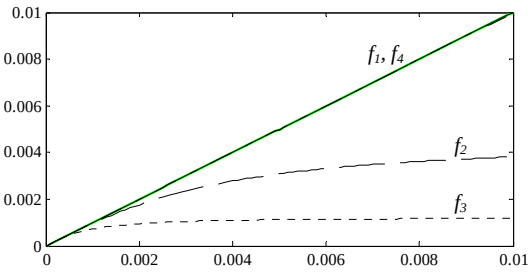

Fig. 7 Optimised saturation functions f_i

These results are typical of a number of variations of the method which were examined, and there are essentially two conclusions which can be drawn. Firstly, Fig. 6 shows that the saturation function in Φ can be successfully optimised to model the progressive saturation effect of the tyres; note that all three steps in a_y are accurately tracked. The cost here used W = I, to bias the optimisation towards accuracy in a_y (since $\dot{r}$ deviations are far lower in magnitude), and the cost was reduced from P = 3.56 for ϕ to P = 0.25 for Φ by the final stage optimisation of $\underline{p}$, $\underline{\beta}$. The result is achieved by paired nonlinearity, such that the state corresponding to one eigenvalue is saturated, whereas that corresponding to its conjugate is not (eqn. (11) and Fig. 7).

However, there is apparently not sufficient freedom in the model structure to allow both outputs to saturate correctly. Fig. 6 shows steady state errors in $\dot{r}$ which can be altered by alternative choices of W, but only to the detriment of performance in a_y. Thus one must conclude that either

(i) the constrained optimisation in Section 2.3 is capable of finding only local minima, and hence an alternative approach to optimisation is required,

or (ii) that separate nonlinearity functions (and hence a separate instance of the simulation model Φ is required for each output.

Given that a range of possible start conditions were examined for $\underline{p}$ and $\underline{\beta}$, it seems unlikely that an alternative optimisation method would present a solution to this problem.

4. TEST VEHICLE EXPERIMENT

Although the simulation experiment reveals limitations to the method, it is still valuable to see the extent to which it can function to compensate the rig delay when approximating a test vehicle's response. Within this section we will restrict attention to the single input / output relationship δ to a_y. Accordingly Fig. 8 shows the first stage, identification of ϕ_h(s), to data acquired from a Jaguar XJ test vehicle.

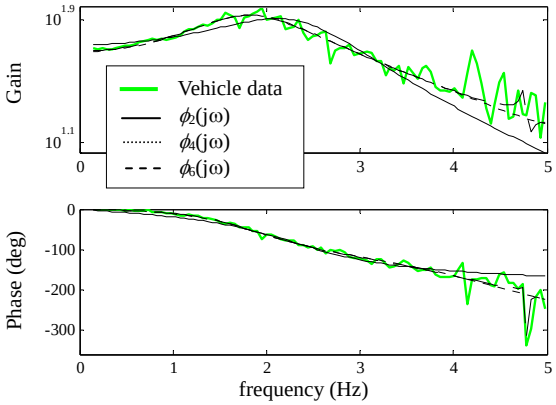

Fig. 8 Identified frequency response functions for vehicle data, orders n = 2, 4, 6

Note first that the fit must be constrained to the range 0-5Hz, since this is the range of valid data from the experiment, given the driver's capability to randomly excite the steering input.

Three choices, n = 2, 4 and 6 are shown, and these illustrate one significant benefit of the staged approach adopted in this paper. We can see by inspection that the 2 state choice is not sufficient to model the combination of vehicle response and delay. Also the 6 state variant is unsuitable; clearly it is under-determined, acting as it does to match a noise corrupted outlier in the data – note the phase fit around 4.8Hz. Conversely, n = 4 provides an excellent compromise.

The linear and nonlinear variants of the vehicle subsystem model are again shown in Fig. 9 – here illustrating also the concatenation of a_{NL} in the first 15 second of data with a_L in the final 5 seconds. (This is the full time history for evaluation of P, eqn (9)).

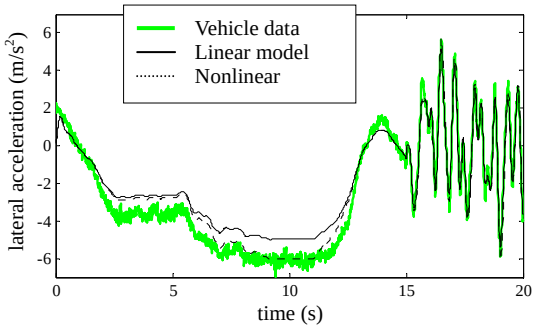

Fig. 9 Combined linear and nonlinear test inputs and identified model performance for vehicle data

We can see that, as with the simulated case, the random steer response between 15 – 20 s is very well matched by the model (here again with n = 4). The performance on this section of the time history is degraded slightly by the fully nonlinear system Φ, but the improvement over the nonlinear section of test data compensates this, with P reducing from 0.723 to 0.366.

Fig. 10 shows an independent section of vehicle test data, with ϕ and Φ compared, and this validates the nonlinear behaviour seen in the optimised section of Fig.

9. Note the staging in the response however, which is clear in both figures, with underestimation of the response between 2 and 7 seconds in Fig. 9. The continuous nonlinear behaviour seen in the simulation study is not fully replicated here.

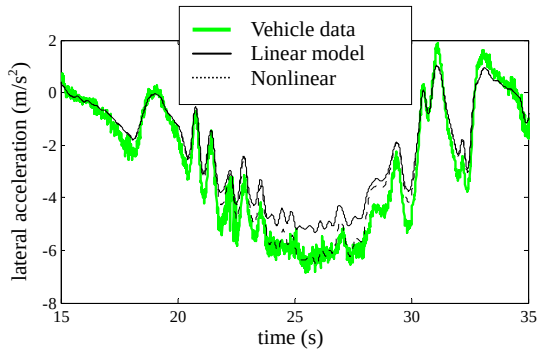

Fig. 10 Identified model performance for vehicle validation data

5. CONCLUSION

The algorithm achieves the principal objective of plant compensation, and successfully optimised subsystem models have been demonstrated for both simulated and test vehicle cases. The method also achieves the five objectives listed in the introduction. By separating linear from nonlinear operation, the relative performance under low and high amplitude conditions are also separated, and the structure enables a degree of confidence that the model will work over a range of inputs. Also, the method allows the required model order to be determined easily by inspection.

The apparent limitation to single input / output systems does present a signficant shortcoming however, and although this can be overcome by running multiple instances of the linear structure with separately optimised nonlinearities, that solution is far from elegant. It must also be conceded that the magnitude of the lag to be compensated, and the level of error induced by tyre nonlinearity are not large for the examples considered; it is recognised that such errors would almost certinaly not be perceived by users of the simulator.

Nevertheless, the method works in principal, and may also find applications elsewhere, since the elements of the algorithm are not specific to the simulator application. Further work on the choice of nonlinearity and the optimisation of its parameters may also yield more widely applicable results.

REFERENCES

[1].Welch, P.D., “The Use of Fast Fourier Transform for the Estimation of Power Spectra: A Method Based on Time Averaging Over Short, Modified Periodograms”, IEEE Trans. Audio Electroacoustics, Vol. AU-15, pp. 70-73 (1967).

[2].Dennis, J.E. and Schnabel, R.B., Numerical Methods for Unconstrained Optimization and Nonlinear Equations, Englewood Cliffs, NJ: Prentice-Hall (1983).

[3].Fletcher, R. and Powell, M.J.D., “A Rapidly Convergent Descent Method for Minimization”, Computer Journal, vol. 6, pp. 23-26, (1963).

[4].Pacejka, H.B., “Tyre and Vehicle Dynamics”, Butterworth Heinemann. (2002).

[5].Gordon, T.J. and Best, M.C., “On the Synthesis of Driver Inputs for the Simulation of Closed-loop Handling Manoeuvres”, International Journal of Vehicle Design, vol 40, pp 52-76 (2006).